Functional genomics implicates natural killer cells in the pathogenesis of ankylosing spondylitis

Marcos Chiñas[1,3], Daniela Fernandez-Salinas[1,3,4], Vitor R. C. Aguiar[1,2,3], Victor E. Nieto-Caballero[1,3,4], Micah Lefton[5], Peter A. Nigrovic[1,2,5], Joerg Ermann*[2,5], Maria Gutierrez-Arcelus*[1,2,3]

1. Division of Immunology, Boston Children's Hospital, Boston, MA, USA.
2. Harvard Medical School, Boston, MA, USA.
3. Program in Medical and Population Genetics, Broad Institute of Harvard and MIT, Cambridge, MA, USA.
4. Licenciatura en Ciencias Genomicas, Centro de Ciencias Genomicas, Universidad Nacional Autónoma de México (UNAM), Morelos 62210, Mexico.
5. Division of Rheumatology, Inflammation and Immunity, Brigham and Women's Hospital, Boston, MA 02115, USA.

*Co-corresponding authors:

Maria Gutierrez-Arcelus
Boston Children's Hospital
Division of Immunology
Karp Family Research Laboratories, Room 102016.1
1 Blackfan Circle
Boston, MA, 02115
mgutierr@broadinstitute.org
857-559-3229

Joerg Ermann
Brigham and Women's Hospital
Division of Rheumatology, Inflammation and Immunity
Hale Building for Transformative Medicine, Room 6002P
60 Fenwood Road
Boston, MA, 02115
jermann@bwh.harvard.edu
617-525-1227

Abstract

Objective: Multiple lines of evidence indicate that ankylosing spondylitis (AS) is a lymphocyte-driven disease. However, which lymphocyte populations are critical in AS pathogenesis is not known. In this study, we aimed to identify the key cell types mediating the genetic risk in AS using an unbiased functional genomics approach.

Methods: We integrated genome-wide association study (GWAS) data with epigenomic and transcriptomic datasets of human immune cells. To quantify enrichment of cell type-specific open chromatin or gene expression in AS risk loci, we used three published methods that have successfully identified relevant cell types in other diseases. We performed co-localization analyses between GWAS risk loci and genetic variants associated with gene expression (eQTL) to find putative target genes.

Results: Natural killer (NK) cell-specific open chromatin regions are significantly enriched in heritability for AS, compared to other immune cell types such as T cells, B cells, and monocytes. This finding was consistent between two AS GWAS. Using RNA-seq data, we validated that genes in AS risk loci are enriched in NK cell-specific gene expression. Using the human Space-Time Gut Cell Atlas, we also found significant upregulation of AS-associated genes predominantly in NK cells. Co-localization analysis revealed four AS risk loci affecting regulation of candidate target genes in NK cells: two known loci, *ERAP1 and TNFRSF1A*, and two under-studied loci, *ENTR1* (aka *SDCCAG3*) and *B3GNT2*.

Conclusion: Our findings suggest that NK cells may play a crucial role in AS development and highlight four putative target genes for functional follow-up in NK cells.

Introduction

Axial spondyloarthritis (axSpA) is a chronic inflammatory rheumatic disease characterized by inflammation of the spine and sacroiliac joints, with a proportion of patients also presenting with arthritis in peripheral joints, uveitis, psoriasis or inflammatory bowel disease (1). Historically, most genetic and pathogenetic studies in axSpA have been carried out in ankylosing spondylitis (AS), a severe and well-characterized subtype of axSpA. The heritability of AS is high, with estimates ranging between 40-90% (2). HLA-B27 is the major risk allele for AS (OR = 21.4) (3). Additionally, genome wide-association studies (GWAS) have revealed >100 non-MHC risk loci for AS, most of them implicating non-coding variants (4–8).

Many immune cell-types have been associated with axSpA (9,10). However, which ones are "driver" cell types actively contributing to the pathogenesis of the disease, as opposed to "bystanders" that become involved as a consequence of the disease, remains unclear. Studies leveraging genetic risk variants and their overlap with epigenomic and transcriptomic features variably suggested CD8+ T cells, CD4+ T cells, NK (natural killer) cells, monocytes, and gastrointestinal cells as potential mediators of AS genetic risk (10–14). However, these studies did not apply the new functional genomics datasets generated from human cells or the latest methodologies designed to integrate functional genomics with GWAS data. This new generation of methods takes advantage of the full range of SNPs examined in a GWAS (not just those surpassing the genome-wide significance threshold) and robustly control for genomic and linkage disequilibrium biases (15–17).

For several immune-mediated diseases, these integrative functional genomics methods have successfully identified specific cell types as drivers of disease development. For example, for rheumatoid arthritis (RA), multiple studies have found a significant enrichment of genetic risk in open or active chromatin regions (marking regulatory elements) specific for T cells (11,18–20). Both mouse and human studies corroborate the role of T cells as central players in RA pathogenesis (21–23). Similarly, for systemic lupus erythematosus (SLE), studies have identified an enrichment of B cell-specific putative regulatory elements and gene expression in SLE risk loci (19,20,24,25) consistent with the well-established role of B cells in SLE pathogenesis (26,27). Hence, there is precedence that the integration of GWAS with functional genomics datasets can identify cellular drivers in inflammatory diseases with complex pathogenesis.

105 Here we sought to investigate which immune cell populations could be drivers of AS development.
106 We integrated GWAS summary statistics from two different AS cohorts with epigenomic and
107 transcriptomic datasets of human leukocytes from peripheral blood and tissue using established
108 methods that control for biases in genomic enrichment analyses. Our results bring forward NK
109 cells as potential key drivers in the pathogenesis of AS.

110 Results

111

112 In order to assess which immune cell types might be mediating the genetic susceptibility to AS,
113 we first utilized a dataset of open chromatin profiles of immune cell subsets from peripheral blood
114 of four healthy subjects (19) (**Fig. 1A**). Sorted cell subsets were analyzed using ATAC-seq with
115 or without prior *in vitro* stimulation. For our study, we grouped the cells analyzed by Calderon et
116 al. into 7 main immune cell types: T cells, B cells, NK cells, plasma cells, dendritic cells (DCs),
117 plasmacytoid DCs, and monocytes. We identified cell type-specific open chromatin regions and
118 assessed whether these were significantly enriched in AS genetic risk. We used the LDSC-SEG
119 method (15) to quantify enrichment of partitioned heritability in each of these cell type-specific
120 annotations (conceptual scheme in **Fig. 1B,** data in **Fig. 1C**) compared to baseline and control
121 annotations, while taking into account the effects of linkage disequilibrium. We excluded the MHC
122 region from our analyses given the unusually high linkage disequilibrium in this region and the
123 fact that genetic associations with this locus are mostly driven by coding variants of the HLA-B
124 gene. Using the Immunochip association study summary statistics from the International Genetics
125 of Ankylosing Spondylitis Consortium (IGAS) (7), we found that NK cell-specific open chromatin
126 regions were significantly enriched in genetic risk for AS (P = 0.026), while this was not the case
127 for the other six immune cell types (**Fig. 1D**).

128

129 We validated this finding in a GWAS with genome-wide genotyping using the summary statistics
130 for AS from the UK Biobank. With this GWAS, we confirmed that open chromatin regions specific
131 for NK cells were significantly enriched in AS heritability (P = 0.034, **Fig. 1E**). To evaluate the
132 reliability of our results, we included four control traits that have been extensively examined in
133 similar studies integrating GWAS with functional genomics (15,18–20). As expected, RA
134 presented the highest enrichment for T cell-specific open chromatin regions (P = 0.0018),
135 Alzheimer's for myeloid DC (P = 0.00018), and SLE for B cells (P = 0.0015). We selected body
136 height as a negative control trait anticipating no significant enrichment for immune cells, a

prediction that was confirmed by our data (all P > 0.1, **Supplementary Fig. 1**). Collectively, these epigenomic analyses suggest that AS risk alleles are preferentially located in regions that may influence gene regulation in NK cells.

To corroborate these findings using an alternative experimental approach, we used our previously published RNA-seq dataset of sorted peripheral CD4+ T, CD8+ T, MAIT, invariant NKT (iNKT), γδ T cells expressing Vδ1 TCR chain (Vd1), γδ T cells expressing Vδ2 TCR chain (Vd2), and NK cells (each in duplicate from 6 healthy donors, **Fig. 2A**) (28). We applied the SNPsea method, which quantifies enrichment of cell type-specific gene expression in risk loci for a given trait (conceptual scheme in **Fig. 2B**) by employing a non-parametric statistical method to calculate empirical P-values through comparison with sets of null SNPs (29). We used the AS risk SNPs reported by Brown and Wordsworth in 2017 which were curated from multiple AS genetic studies (30). SNPsea analysis revealed a significant enrichment of NK cell-specific gene expression in AS risk loci (P = 0.01), which was not observed in the other lymphocyte subsets included in the dataset (**Fig. 2C**).

We then performed a differential expression analysis comparing NK cells with the six T cell subsets (Supplementary Table 1). Genes in AS risk loci with significant upregulation in NK cells are presented in **Fig 2D**. Two of these genes, *RUNX3* and *TBX21* (Tbet), encode transcription factors with important roles in lymphocytes. *TNFRSF1A* encoding TNF Receptor I has a well-established association with AS that has been validated by multiple studies (31–33). *FCGR2A* codes for the low-affinity Fcγ receptor IIA, an activating receptor involved in orchestrating immune response. Less studied genes included *NPEPPS,* which encodes a puromycin-sensitive aminopeptidase, and *LNPEP*, which encodes a zinc-dependent aminopeptidase (34). Both genes are paralogs of *ERAP1* and belong to the MHC Class I antigen processing and presentation pathway, along with other known AS risk genes (35–37). Collectively, the results of our second integrative analysis indicate that several genes within AS risk loci are highly expressed in NK cells relative to T cells, providing additional support for the emerging hypothesis that AS risk alleles exert their effects, at least in part, via NK cells.

The transcriptomic phenotype of immune cells commonly differs between blood and tissue (38–41). Hence, in addition to analyzing peripheral blood as in the previous analyses, we sought to evaluate disease-relevant cell subsets from a tissue relevant for AS. We used the human Space-

170 Time Gut Cell Atlas (42) which includes scRNA-seq data for samples from various locations of
171 fetal (N = 16), pediatric (N = 8) and adult (N = 13, including 6 healthy and 7 Crohn's disease
172 patients) intestine (**Fig. 3A)**. We applied the scDRS method (16) which identifies cells that over-
173 express a significant proportion of genes implicated by GWAS, weighted on their strength of
174 association with disease, compared to null sets of control genes in the dataset (conceptual
175 scheme in **Fig. 3B**). The Space-Time Gut Cell Atlas investigators identified the following broad
176 cell types: mesenchymal, epithelial, endothelial, neuronal, myeloid, red blood cells, B cells,
177 plasma cells, T cells, NK cells and other innate lymphoid cells (ILCs)(**Fig. 3C)**. scDRS identified
178 1,852 cells with significantly enriched expression of AS GWAS genes (20% FDR, **Fig. 3D**). Of
179 these, 765 were T cells, 264 myeloid cells, 320 NK cells and 319 other ILCs. Normalized for cell
180 type abundance in the dataset, NK cells showed the highest enrichment (39-fold), followed by
181 other ILCs (34-fold), T cells (5-fold), and myeloid cells (5-fold, **Fig. 3E**). In contrast, non-immune
182 cell types exhibited a depletion of disease relevant cells relative to their abundance in the entire
183 dataset (**Supplementary Fig. 2**). We then used the fine-grained annotations of the Space-Time
184 Gut Cell Atlas to identify the particular cell subsets that had significant expression enrichment of
185 AS-associated genes. This revealed NK cells as the most abundant (N = 320), followed by Lti-
186 like NCR+ ILC3 cells (N = 147), activated CD8+ T cells (N = 132), macrophages (N = 130), Lti-
187 like NCR- ILC3 cells (N = 112), $\gamma\delta$ T cells (N = 94), and other T cells, ILCs and myeloid subsets
188 (**Fig. 3F**). Genes in AS risk loci with high expression in gut NK cells include *GNLY*, *CCL4* and
189 *CCL3* (**Fig. 3G**). Using the control traits specified earlier, we confirmed T cells as the main
190 disease-relevant cell type for RA and monocytes for Alzheimer's disease (**Supplementary Fig.
191 2**). No significant disease-relevant cells were identified for height (as expected) and for SLE,
192 which could mean that B cells in the gut are in a state not pertinent to SLE or that the dataset
193 lacked sufficient power to detect an association for this disease (**Supplementary Fig. 2**). In sum,
194 our analyses indicate that tissue-resident NK cells exhibit significant expression of AS-associated
195 genes.
196
197 Lastly, we sought to find putative target genes for AS risk variants in NK cells. To this end we
198 performed co-localization analyses between AS GWAS risk loci and genetic variants associated
199 with gene expression (expression quantitative trait loci, eQTLs) using coloc (43). We leveraged
200 eQTL summary statistics from the eQTL Catalogue (44) drawing upon data from a study on the
201 transcriptomic profiling of peripheral NK cells from 91 genotyped individuals (45) as well as a
202 microarray QTL study that profiled NK cells from 245 genotyped individuals (46). We found four
203 AS risk loci with genome-wide significance ($P < 5 \times 10^{-8}$) and a high posterior probability (>0.8) of

204 sharing a causal variant with an NK cell eQTL (PP4, **Table 1, Fig. 4**). An additional 10 loci with
205 suggestive AS association P-values ($3.56 \times 10^{-5} < P < 5.40 \times 10^{-8}$) showed evidence of co-
206 localization with NK cell eQTLs for 18 genes (PP4 > 0.75, **Table 1**). Within the genome-wide
207 significant loci we identified the established target genes *ERAP1* and *TNFRSF1A*, as well as the
208 putative target genes *ENTR1* (a.k.a. *SDCCAG3*) and *B3GNT2*, which have been studied less.
209

210 ## Discussion

211

212 In this study we integrated epigenomic and transcriptomic datasets with AS genetic risk data to
213 find candidate cellular drivers of AS pathogenesis. Our unbiased approach, applying three
214 different methods to datasets from both peripheral blood and tissue, consistently identified NK
215 cells as the dominant disease-relevant cell type. Specifically, we found that NK-specific open
216 chromatin regions and NK-specific gene expression were significantly enriched for non-MHC AS
217 genetic risk. This suggests that a significant portion of AS risk variants affect gene regulation in
218 NK cells, pointing to NK cells as potential key mediators of AS pathogenesis.
219

220 NK cells have the ability to directly destroy target cells through cell lysis, and in addition play a
221 significant role in shaping immune responses by releasing cytokines (47). Previous studies
222 support a role for NK cells in AS. AS patients with chronic subclinical intestinal inflammation were
223 found to have an increased abundance of NKp44+ NK cells in their gut, and these cells were the
224 major producers of IL-22 in the lamina propria, suggesting a possible role in tissue protection (48).
225 One could speculate that dysfunctional NK cells “drive” AS development by contributing to
226 intestinal inflammation, in line with the gut-joint axis hypothesis (49). Alternatively, NK cells may
227 play a critical role through activities in spinal tissues. Cuthbert *et al.* studied entheseal immunology
228 using discarded surgical specimens from patients with back pain (not axSpA) undergoing
229 laminectomy and reported that NK cells are present in both entheseal soft tissue and peri-
230 entheseal bone (50). We are not aware of any data assessing the presence of NK cells at spinal
231 enthesis in AS patients or in the subchondral bone marrow in patients with sacroiliitis.
232

233 HLA-B27 can bind to the killer cell immunoglobulin-like receptor (KIR) KIR3DL1 and affect the
234 function of NK cells, including their ability to lyse cells (51–53). HLA-B27 homodimers can also
235 bind KIR3DL2 (54). Chan and colleagues showed an expansion of KIR3DL2+ NK and CD4+ T
236 cells in AS patients (Chan Arthritis Rheum 2005, PMID 16255049). Subsequent studies by the
237 same group focused on CD4+ T cells demonstrating that KIR3DL2+ CD4+ T cells were major IL-

238 17A producers (55). However, an expansion of KIR3DL2+ NK and T cells has not been observed
239 in other axSpA cohorts (56,57). Multiple risk loci for AS include genes relevant for NK cell function,
240 including *KIR2DL1*, *KIR3DL1*, *KIR2DS5*, *KIR3DS1* and *KIR2DL5* (58–62). In another study,
241 investigators co-cultured ERAP1-inhibited M1 macrophages with NK cells from AS patients, and
242 found that patients with ERAP1 protective alleles led to decreased CD69 and CD107a on NK cells
243 and a lower number of IFN-γ+ NK cells compared to patients carrying non-protective alleles (63).
244
245 Our findings do not rule out the involvement of other cell types in AS pathogenesis. Indeed, in the
246 human Space-Time Gut Cell Atlas, we identified significant expression of AS-associated genes
247 in T cell subsets and ILC subsets (Fig. 3D-F), which share transcriptional programs with NK cells
248 (28,64–66). Indeed, it is likely that genetic risk to AS is mediated through multiple cell types, as is
249 the case for other complex diseases such as multiple sclerosis, for which studies have found risk
250 enrichment in open/active chromatin regions specific to both T cells and B cells (20). We and
251 others have shown that eQTLs often exhibit impact in multiple cell types (67,68). Hence,
252 determining the specific cell type through which a disease risk variant is exerting its pathogenic
253 effects can be challenging.
254
255 Our co-localization analyses using two eQTL NK cell datasets identified four putative target genes
256 for AS risk variants: *ERAP1*, *TNFRSF1A*, *ENTR1* (a.k.a. *SDCCAG3*) and *B3GNT2*. The
257 importance of *ERAP1* in AS risk is well established, and polymorphisms affecting its expression
258 have been reported for multiple cell types, including macrophages, monocytes, T cells, and
259 induced pluripotent stem cells, fibroblasts, and immortalized B cells (69–71). Similarly, multiple
260 studies have found significant associations between non-coding polymorphisms at or near
261 *TNFRSF1A* and AS, including in European and East Asian populations (31,32,72,73). While there
262 are multiple genes in this genomic locus, including *PLEKHG6*, *SCNN1A*, and *LTBR*, our co-
263 localization results suggest that *TNFRSF1A*, which encodes TNF receptor I, is the target gene of
264 the causal variant in this locus, and its dysregulation can happen in NK cells. This is consistent
265 with the therapeutic efficacy of TNF inhibitors in AS and the known function of TNF as a booster
266 of the cytolytic capacity of NK cells (74). Interestingly, TNFRSF1A has been functionally linked to
267 ENTR1, a less extensively studied putative target gene identified in this study. *ENTR1*, which
268 encodes an endosome-associated trafficking regulator, is needed for TNF receptor expression on
269 the cell surface (75). Lastly, *B3GNT2* encodes an acetylglucosaminyltransferase enzyme that is
270 a type II transmembrane protein. A recent study in a Taiwanese cohort demonstrated that a non-
271 coding genetic variant near *B3GNT2* is associated with AS susceptibility, and that *B3GNT2* blood

272 mRNA levels were negatively correlated with C-reactive protein (CRP), erythrocyte sedimentation
273 rate, syndesmophyte formation, and Bath ankylosing spondylitis functional index (BASFI) (76).
274
275 While the 4 putative target genes identified here make sense in the context of AS and potential
276 impact on NK cell function, they are not as numerous as we would have expected given the 32
277 genome-wide significant risk loci included in the co-localization analyses. However, similar
278 challenges have been encountered with non-coding risk variants in other complex diseases,
279 where only 20-47% of risk variants co-localized with eQTLs (77–79). Our research, along with
280 that of others, suggests that many regulatory effects might remain undetected due to their
281 presence in cell states of activation or differentiation that have not been thoroughly explored (80–
282 83). Moreover, the sample size of typical eQTL studies is likely insufficient to find the regulatory
283 effects of most risk variants identified by GWAS (84). Hence, we believe that better-powered
284 eQTL studies ascertaining multiple activation states in NK cells are needed to find additional
285 target genes for AS risk variants.
286
287 One limitation of our study, due to a lack of published data, is the incomplete assessment of the
288 spectrum of potentially relevant immune cell subsets and states, particularly those present in
289 inflamed sacroiliac joints and spine. Consequently, if the real driver for AS pathogenesis is a cell
290 subset or state that was not present in the analyzed datasets, but has transcriptomic and
291 epigenomic similarities to NK cells, then our results may suffer from “guilt-by-association” bias.
292 To our knowledge, current transcriptomic datasets profiling multiple immune cell types from AS
293 patients are limited to peripheral blood (14,85–90). When we applied scDRS to a recently
294 published single-cell RNA-seq dataset of 98,884 PBMCs cells from 10 AS patients and 29 healthy
295 controls (88), we found no significant cells for the disease-relevant gene expression score (data
296 not shown), possibly due to lack of power in the study for this type of analysis.
297
298 Our study encompassed a broad spectrum of immune cell states within the gastrointestinal tract
299 and peripheral blood of healthy subjects and consistently pointed to NK cells. Since GWAS
300 pinpoint genetic regions implicated in the onset of disease, including early stages when future
301 patients are still asymptomatic, the study of samples from healthy subjects is relevant, despite
302 the possibility that not all cell states are represented. Future investigations, particularly larger-
303 scale studies of samples from blood and inflamed tissue from AS patients including untreated
304 patients in the early phases of the disease, will be key to establish whether NK cells are indeed
305 drivers of AS pathogenesis.

306

307 ## Materials and Methods

308 ### Genome-wide association studies

309 We used the GWAS ImmunoChip summary statistics from the International Genetics of
310 Ankylosing Spondylitis Consortium (IGAS). The IGAS study, led by (7), performed high-density
311 genotyping of 9,069 AS cases and 13,578 healthy controls. In addition, we used the GWAS
312 summary statistics from the UK Biobank, which involved a case-control design with 1,185 AS
313 cases and 419,276 controls, providing genome-wide coverage for AS susceptibility loci (91).
314
315 We lifted the genomic positions of the genetic variants to genome build hg19 or hg38 according
316 to the version compatible with subsequent analyses. Given the complexity and strong genetic
317 association signals within the Major Histocompatibility Complex (MHC) region, we excluded
318 variants located on chr6:25,000,000–34,000,000.
319
320 We additionally used GWAS summary statistics for rheumatoid arthritis, Alzheimer's disease, and
321 systemic lupus erythematosus as positive control traits for which we know the disease relevant
322 immune cell types, and height as a negative control trait for which we do not expect immune cells
323 to be relevant. The summary statistics for control traits were preprocessed by the Alkes Price
324 laboratory, they included HapMap 3 SNPs and SNPs that are in the 1000 Genomes Project, and
325 they excluded the MHC region (chr6:25Mb-34Mb). These summary statistics are available at
326 https://alkesgroup.broadinstitute.org/.
327

328 ### Epigenomic and transcriptomic datasets

329 To identify cell type-specific open chromatin regions in different immune cell types, we used the
330 Calderon *et al.* study *(19)*, in which the authors collected blood from 4 healthy subjects, sorted
331 immune cell types, and generated chromatin accessibility profiles using Assay for Transposase-
332 Accessible Chromatin sequencing (ATAC-seq, GSE118189).
333
334 To find AS risk enrichment for cell type-specific expression, we incorporated data from the study
335 conducted by Gutierrez-Arcelus *et al.* (28), which involved low-input mRNA-seq data from sorted

336 NK cells and six T cell subsets isolated from 6 healthy subjects (each with two replicates per cell-
337 type, GSE124731).
338
339 We used the Space-Time Gut Cell Atlas to identify cells exhibiting significant upregulation of
340 disease-associated genes. This dataset includes single-cell RNA-seq profiling of 428,000
341 intestinal cells obtained from fetal (N = 16), pediatric (N = 8), and adult donors (N = 13). The
342 dataset covers 11 different intestinal regions (42), https://www.gutcellatlas.org/.
343

344 **Differential accessibility analysis**

345 We used the counts of open chromatin consensus peaks called by Calderon et al. First, we
346 transformed counts into Reads Per Kilobase per Million mapped reads (RPKM), then normalized
347 by quantiles using the preprocess Core R package and finally scaled to their log2 (normalized
348 RPKM+1), thus we account for differences in library size across samples and peak length
349 variability. We pooled sorted samples into 7 main immune cell types, aiming for a similar number
350 of samples per cell type to avoid biases in the differential accessibility analyses: T cells (stimulated
351 and unstimulated CD8+ T, unstimulated naïve CD4 T and memory CD4 T), B cells (stimulated
352 and unstimulated bulk B cells, unstimulated memory and naïve B cells), natural killer cells
353 (stimulated and unstimulated mature NKs, unstimulated memory NK and immature NK cells),
354 monocytes (stimulated and unstimulated monocytes), plasma cells (unstimulated plasma cells),
355 dendritic cells (unstimulated myeloid DCs), plasma dendritic cells (unstimulated plasmacytoid
356 DCs). The latter three cell-types had less samples available, however, this did not impede our
357 control trait Alzheimer disease to show significant heritability enrichment for myeloid DC-specific
358 open chromatin regions, as expected (see Methods below and main text).
359
360 Next, we employed linear mixed model regression to identify regions that exhibited differential
361 accessibility between each cell type and the rest of the cell types. To account for potential donor-
362 specific effects, we incorporated the donor ID variable as a random effect in our analysis.
363 For each cell type comparison, we tested peaks that had counts greater than the mean for that
364 cell type in at least half of the samples, this yielded between 400 to 600 thousand tested peaks
365 depending on the cell type. To select the “cell type-specific open chromatin peaks” for each cell
366 type, we sorted open chromatin peaks by their t-statistic and chose the positive top 10%.

367 **Partitioned heritability enrichment analysis with LDSC-SEG**

368 Linkage Disequilibrium score regression applied to specifically expressed genes (LDSC-SEG)
369 v1.0.1 method was applied to determine disease-relevant cell types (15,92) for AS.
370
371 Cell type-specific open chromatin peaks were extended by 225bp to each side, to match the
372 genomic coverage recommended by the LDSC-SEG authors. These annotations were then
373 utilized as input for the partitioned heritability enrichment analysis by LDSC-SEG. We used the
374 baseline annotation v1.2 provided by Price Lab for LDSC-SEG, comprising 75 background
375 annotations. Additionally, we used all consensus peaks (N = 829,942) of Calderon et al. as the
376 control annotation. Using other baselines or controls did not affect our results. We utilized SNP
377 weight files derived from the HapMap 3 project (HM3) European population.
378

379 **Analysis of cell type-specific gene expression enrichment in risk loci using SNPsea**

380 SNPsea analysis aimed to assess the association between risk SNPs and genes expressed
381 specifically for a given cell type (29). We incorporated a curated list of risk SNPs for ankylosing
382 spondylitis (AS), compiled by Brown and Wordsowrth 2017 (30), which includes genetic variants
383 that have been associated with AS susceptibility. This list was derived from multiple AS studies
384 conducted until 2017.
385 We utilized the expression data obtained from Gutierrez-Arcelus et al. (2019). The gene
386 expression counts in this dataset were normalized to transcripts per million (TPM) and
387 transformed to log2(TPM+1) values. To identify the genes with meaningful expression levels, we
388 included those with log2(TPM+1) > 2 in at least 10 samples. SNPsea was then run for the
389 normalized expression matrix and AS risk SNPs, using recombination intervals from Myers et al.
390 (93), null SNPs from Lango et al. (94), and the following parameters: --score single --slop 10000
391 --threads 2 --null-snpsets 0 --min-observations 100 --max-iterations 10000000.
392

393 **Integration of GWAS with single-cell RNA-seq with scDRS**

394 We used the single-cell Disease Relevance Score (scDRS) by combining scRNA-seq and GWAS
395 to identify cells with significant up-regulation of disease-associated genes, which are scored
396 based on their strength of association with disease, and are compared with null sets of genes
397 present in the dataset.

As recommended by scDRS authors, we first created disease-relevant genesets using Multi-marker Analysis of GenoMic Annotation (MAGMA) version 1.10 (95). First, we generated gene annotations with MAGMA setting a window of 10kb using the following parameters: "--annotate window=10,10 --snp-loc ./g1000_eur/g1000_eur.bim --gene-loc ./NCBI37.3/NCBI37.3.gene.loc". Then we ran MAGMA using GWAS summary statistics for traits of interest with the following parameters: --bfile ./magma_v1.10/g1000_eur/g1000_eur --pval GWAS.pval use='SNP,P' ncol='N' --gene-annot ./magma_v1.10/out/step1.genes.annot.

We ran scDRS using the disease-relevant gene sets from MAGMA, the expression data obtained from the Space-Time Gut Cell Atlas (42) and corrected for biases by adding as covariates the number of genes expressed per cell and sample batch. Next, for visualization purposes and downstream analysis, we processed the single-cell dataset using Seurat (96), we performed integration across batches with Harmony (97), and we visualized cells in two dimensions with Uniform Manifold Approximation and Projection (UMAP). We labeled cells plotted in UMAP by the annotations defined by the Space-Time Gut Cell Atlas. Additionally, we colored cells by their scDRS score when cells passed the 0.20 FDR threshold.

eQTL co-localization analysis

To select genomic loci for colocalization analysis, GWAS summary statistics were sorted by P-values, then starting from the variant with the smallest P-value, variants within a 50 Kb window were removed. The process was repeated with the next most significant variant among the remaining variants until no variant with a P-value below 5×10^{-5} was left. We performed colocalization analysis for GWAS studies against the eQTL Catalogue (44). We imported eQTL summary statistics from RNA-seq and microarray from Schmiedel et al. (45) and Gilchrist et al. (2022). We fetched the summary statistics data using the tabix method with the seqminer R package (v8.5). For each region tested, we included all biallelic SNPs that were ascertained in both the GWAS and eQTL study and performed the analysis only for genes within a window of ±500,000 base pairs from the GWAS top variant, and for which there was at least one eQTL passing the 5×10^{-5} P-value threshold. Before merging GWAS and QTL data, the variant coordinates of the GWAS were lifted to the GRCh38 version of the reference genome using liftOver with the UCSC chain file. We used the coloc v5.1.0.1 package (98) in R v4.1.0 to test for colocalization at each gene and dataset. The code is available at <https://github.com/gutierrez-arcelus-lab/>.

Each locus was plotted using plotgardener (99), and we recovered the LD of the top SNP in a given region in the GWAS dataset using the locuscomparer package (100). Then we used plotgardener functions to display the regions near the lead variant and colored the genes tested using the posterior probability that the two traits share a causal variant (PP4).

Data availability

All data and methods are publicly available as specified above.

Acknowledgments

This study was supported by a seed grant from the Spondyloarthritis Research and Treatment Network (SPARTAN) and a microgrant from the Joint Biology Consortium (1P30AR070253-01). PAN was supported by P30AR070253 and R01AR073201. JE was supported by NIH Grant R21 AR076040-01 and an ASPIRE grant from Pfizer. MGA was supported by P30AR070253, the Arthritis National Research Foundation, the Lupus Research Alliance, and the Gilead Sciences Rheumatology Research Scholars Award. We thank Soumya Raychaudhuri and Kamil Slowikowski for guidance on implementing SNPsea, and Steven Gazal for guidance on implementing LDSC-SEG. We thank the Gutierrez-Arcelus and Nigrovic laboratories for feedback on this study.

Disclosures

The authors declare they have no relevant conflicts of interest.

References

1. Navarro-Compán V, Sepriano A, El-Zorkany B, Heijde D van der. Axial spondyloarthritis. *Ann Rheum Dis* 2021;80:1511–1521. Available at: http://dx.doi.org/10.1136/annrheumdis-2021-221035.

2. Díaz-Peña R, Castro-Santos P, Durán J, Santiago C, Lucia A. The Genetics of Spondyloarthritis. *J Pers Med* 2020;10. Available at: http://dx.doi.org/10.3390/jpm10040151.

3. Reveille JD, Zhou X, Lee M, Weisman MH, Yi L, Gensler LS, et al. HLA class I and II alleles in susceptibility to ankylosing spondylitis. *Ann Rheum Dis* 2019;78:66–73. Available at: http://dx.doi.org/10.1136/annrheumdis-2018-213779.

464 4. Wellcome Trust Case Control Consortium, Australo-Anglo-American Spondylitis Consortium
465 (TASC), Burton PR, Clayton DG, Cardon LR, Craddock N, et al. Association scan of 14,500
466 nonsynonymous SNPs in four diseases identifies autoimmunity variants. *Nat Genet*
467 2007;39:1329–1337. Available at: http://dx.doi.org/10.1038/ng.2007.17.

468 5. Australo-Anglo-American Spondyloarthritis Consortium (TASC), Reveille JD, Sims A-M, Danoy
469 P, Evans DM, Leo P, et al. Genome-wide association study of ankylosing spondylitis identifies
470 non-MHC susceptibility loci. *Nat Genet* 2010;42:123–127. Available at:
471 http://dx.doi.org/10.1038/ng.513.

472 6. Evans DM, Spencer CCA, Pointon JJ, Su Z, Harvey D, Kochan G, et al. Interaction between
473 ERAP1 and HLA-B27 in ankylosing spondylitis implicates peptide handling in the mechanism for
474 HLA-B27 in disease susceptibility. *Nat Genet* 2011;43:761–767. Available at:
475 http://dx.doi.org/10.1038/ng.873.

476 7. International Genetics of Ankylosing Spondylitis Consortium (IGAS), Cortes A, Hadler J,
477 Pointon JP, Robinson PC, Karaderi T, et al. Identification of multiple risk variants for ankylosing
478 spondylitis through high-density genotyping of immune-related loci. *Nat Genet* 2013;45:730–738.
479 Available at: http://dx.doi.org/10.1038/ng.2667.

480 8. Ellinghaus D, Jostins L, Spain SL, Cortes A, Bethune J, Han B, et al. Analysis of five chronic
481 inflammatory diseases identifies 27 new associations and highlights disease-specific patterns at
482 shared loci. *Nat Genet* 2016;48:510–518. Available at: http://dx.doi.org/10.1038/ng.3528.

483 9. Mauro D, Simone D, Bucci L, Ciccia F. Novel immune cell phenotypes in spondyloarthritis
484 pathogenesis. *Semin Immunopathol* 2021;43:265–277. Available at:
485 http://dx.doi.org/10.1007/s00281-021-00837-0.

486 10. Li Z, Haynes K, Pennisi DJ, Anderson LK, Song X, Thomas GP, et al. Epigenetic and gene
487 expression analysis of ankylosing spondylitis-associated loci implicate immune cells and the gut
488 in the disease pathogenesis. *Genes Immun* 2017;18:135–143. Available at:
489 http://dx.doi.org/10.1038/gene.2017.11.

490 11. Farh KK-H, Marson A, Zhu J, Kleinewietfeld M, Housley WJ, Beik S, et al. Genetic and
491 epigenetic fine mapping of causal autoimmune disease variants. *Nature* 2015;518:337–343.
492 Available at: http://dx.doi.org/10.1038/nature13835.

493 12. Costantino F, Breban M, Garchon H-J. Genetics and Functional Genomics of
494 Spondyloarthritis. *Front Immunol* 2018;9:2933. Available at:
495 http://dx.doi.org/10.3389/fimmu.2018.02933.

496 13. Yazar S, Alquicira-Hernandez J, Wing K, Senabouth A, Gordon MG, Andersen S, et al. Single-
497 cell eQTL mapping identifies cell type-specific genetic control of autoimmune disease. *Science*
498 2022;376:eabf3041. Available at: http://dx.doi.org/10.1126/science.abf3041.

499 14. Brown AC, Cohen CJ, Mielczarek O, Migliorini G, Costantino F, Allcock A, et al.
500 Comprehensive epigenomic profiling reveals the extent of disease-specific chromatin states and
501 informs target discovery in ankylosing spondylitis. *Cell Genom* 2023;3:100306. Available at:
502 http://dx.doi.org/10.1016/j.xgen.2023.100306.

503 15. Finucane HK, Reshef YA, Anttila V, Slowikowski K, Gusev A, Byrnes A, et al. Heritability
504 enrichment of specifically expressed genes identifies disease-relevant tissues and cell types. *Nat*

Genet 2018;50:621–629. Available at: http://dx.doi.org/10.1038/s41588-018-0081-4.

16. Zhang MJ, Hou K, Dey KK, Sakaue S, Jagadeesh KA, Weinand K, et al. Polygenic enrichment distinguishes disease associations of individual cells in single-cell RNA-seq data. *Nat Genet* 2022;54:1572–1580. Available at: http://dx.doi.org/10.1038/s41588-022-01167-z.

17. Jagadeesh KA, Dey KK, Montoro DT, Mohan R, Gazal S, Engreitz JM, et al. Identifying disease-critical cell types and cellular processes by integrating single-cell RNA-sequencing and human genetics. *Nat Genet* 2022;54:1479–1492. Available at: http://dx.doi.org/10.1038/s41588-022-01187-9.

18. Trynka G, Sandor C, Han B, Xu H, Stranger BE, Liu XS, et al. Chromatin marks identify critical cell types for fine mapping complex trait variants. *Nat Genet* 2013;45:124–130. Available at: http://dx.doi.org/10.1038/ng.2504.

19. Calderon D, Nguyen MLT, Mezger A, Kathiria A, Müller F, Nguyen V, et al. Landscape of stimulation-responsive chromatin across diverse human immune cells. *Nat Genet* 2019;51:1494–1505. Available at: http://dx.doi.org/10.1038/s41588-019-0505-9.

20. Soskic B, Cano-Gamez E, Smyth DJ, Rowan WC, Nakic N, Esparza-Gordillo J, et al. Chromatin activity at GWAS loci identifies T cell states driving complex immune diseases. *Nat Genet* 2019;51:1486–1493. Available at: http://dx.doi.org/10.1038/s41588-019-0493-9.

21. Banerjee S, Webber C, Poole AR. The induction of arthritis in mice by the cartilage proteoglycan aggrecan: roles of CD4+ and CD8+ T cells. *Cell Immunol* 1992;144:347–357. Available at: http://dx.doi.org/10.1016/0008-8749(92)90250-s.

22. Kobezda T, Ghassemi-Nejad S, Mikecz K, Glant TT, Szekanecz Z. Of mice and men: how animal models advance our understanding of T-cell function in RA. *Nat Rev Rheumatol* 2014;10:160–170. Available at: http://dx.doi.org/10.1038/nrrheum.2013.205.

23. Rao DA, Gurish MF, Marshall JL, Slowikowski K, Fonseka CY, Liu Y, et al. Pathologically expanded peripheral T helper cell subset drives B cells in rheumatoid arthritis. *Nature* 2017;542:110–114. Available at: http://dx.doi.org/10.1038/nature20810.

24. Hu X, Kim H, Stahl E, Plenge R, Daly M, Raychaudhuri S. Integrating autoimmune risk loci with gene-expression data identifies specific pathogenic immune cell subsets. *Am J Hum Genet* 2011;89:496–506. Available at: http://dx.doi.org/10.1016/j.ajhg.2011.09.002.

25. Khunsriraksakul C, Li Q, Markus H, Patrick MT, Sauteraud R, McGuire D, et al. Multi-ancestry and multi-trait genome-wide association meta-analyses inform clinical risk prediction for systemic lupus erythematosus. *Nat Commun* 2023;14:668. Available at: http://dx.doi.org/10.1038/s41467-023-36306-5.

26. Caielli S, Wan Z, Pascual V. Systemic Lupus Erythematosus Pathogenesis: Interferon and Beyond. *Annu Rev Immunol* 2023;41:533–560. Available at: http://dx.doi.org/10.1146/annurev-immunol-101921-042422.

27. Vinuesa CG, Shen N, Ware T. Genetics of SLE: mechanistic insights from monogenic disease and disease-associated variants. *Nat Rev Nephrol* 2023. Available at: http://dx.doi.org/10.1038/s41581-023-00732-x.

544 28. Gutierrez-Arcelus M, Teslovich N, Mola AR, Polidoro RB, Nathan A, Kim H, et al. Lymphocyte
545 innateness defined by transcriptional states reflects a balance between proliferation and effector
546 functions. *Nat Commun* 2019;10:687. Available at: http://dx.doi.org/10.1038/s41467-019-08604-
547 4.

548 29. Slowikowski K, Hu X, Raychaudhuri S. SNPsea: an algorithm to identify cell types, tissues
549 and pathways affected by risk loci. *Bioinformatics* 2014;30:2496–2497. Available at:
550 http://dx.doi.org/10.1093/bioinformatics/btu326.

551 30. Brown MA, Wordsworth BP. Genetics in ankylosing spondylitis - Current state of the art and
552 translation into clinical outcomes. *Best Pract Res Clin Rheumatol* 2017;31:763–776. Available at:
553 https://www.sciencedirect.com/science/article/pii/S1521694218300548.

554 31. Davidson SI, Liu Y, Danoy PA, Wu X, Thomas GP, Jiang L, et al. Association of STAT3 and
555 TNFRSF1A with ankylosing spondylitis in Han Chinese. *Ann Rheum Dis* 2011;70:289–292.
556 Available at: http://dx.doi.org/10.1136/ard.2010.133322.

557 32. Karaderi T, Pointon JJ, Wordsworth TWH, Harvey D, Appleton LH, Cohen CJ, et al. Evidence
558 of genetic association between TNFRSF1A encoding the p55 tumour necrosis factor receptor,
559 and ankylosing spondylitis in UK Caucasians. *Clin Exp Rheumatol* 2012;30:110–113. Available
560 at: https://www.ncbi.nlm.nih.gov/pubmed/22272576.

561 33. Sode J, Bank S, Vogel U, Andersen PS, Sørensen SB, Bojesen AB, et al. Genetically
562 determined high activities of the TNF-alpha, IL23/IL17, and NFkB pathways were associated with
563 increased risk of ankylosing spondylitis. *BMC Med Genet* 2018;19:165. Available at:
564 http://dx.doi.org/10.1186/s12881-018-0680-z.

565 34. Robinson PC, Brown MA. Genetics of ankylosing spondylitis. *Mol Immunol* 2014;57:2–11.
566 Available at: http://dx.doi.org/10.1016/j.molimm.2013.06.013.

567 35. Vitulano C, Tedeschi V, Paladini F, Sorrentino R, Fiorillo MT. The interplay between HLA-B27
568 and ERAP1/ERAP2 aminopeptidases: from anti-viral protection to spondyloarthritis. *Clin Exp*
569 *Immunol* 2017;190:281–290. Available at: http://dx.doi.org/10.1111/cei.13020.

570 36. Tsui FW, Tsui HW, Akram A, Haroon N, Inman RD. The genetic basis of ankylosing
571 spondylitis: new insights into disease pathogenesis. *Appl Clin Genet* 2014;7:105–115. Available
572 at: http://dx.doi.org/10.2147/TACG.S37325.

573 37. Agrawal N, Brown MA. Genetic associations and functional characterization of M1
574 aminopeptidases and immune-mediated diseases. *Genes Immun* 2014;15:521–527. Available at:
575 http://dx.doi.org/10.1038/gene.2014.46.

576 38. Szabo PA, Levitin HM, Miron M, Snyder ME, Senda T, Yuan J, et al. Single-cell
577 transcriptomics of human T cells reveals tissue and activation signatures in health and disease.
578 *Nat Commun* 2019;10:1–16. Available at: https://www.nature.com/articles/s41467-019-12464-3.
579 Accessed August 4, 2023.

580 39. Meininger I, Carrasco A, Rao A, Soini T, Kokkinou E, Mjösberg J. Tissue-Specific Features of
581 Innate Lymphoid Cells. *Trends Immunol* 2020;41:902–917. Available at:
582 http://dx.doi.org/10.1016/j.it.2020.08.009.

583 40. Domínguez Conde C, Xu C, Jarvis LB, Rainbow DB, Wells SB, Gomes T, et al. Cross-tissue

584 immune cell analysis reveals tissue-specific features in humans. *Science* 2022;376:eabl5197.
585 Available at: http://dx.doi.org/10.1126/science.abl5197.

586 41. Mass E, Nimmerjahn F, Kierdorf K, Schlitzer A. Tissue-specific macrophages: how they
587 develop and choreograph tissue biology. *Nat Rev Immunol* 2023:1–17. Available at:
588 http://dx.doi.org/10.1038/s41577-023-00848-y.

589 42. Elmentaite R, Kumasaka N, Roberts K, Fleming A, Dann E, King HW, et al. Cells of the human
590 intestinal tract mapped across space and time. *Nature* 2021;597:250–255. Available at:
591 http://dx.doi.org/10.1038/s41586-021-03852-1.

592 43. Wang G, Sarkar A, Carbonetto P, Stephens M. A simple new approach to variable selection
593 in regression, with application to genetic fine mapping. *J R Stat Soc Series B Stat Methodol*
594 2020;82:1273–1300. Available at: http://dx.doi.org/10.1111/rssb.12388.

595 44. Kerimov N, Hayhurst JD, Peikova K, Manning JR, Walter P, Kolberg L, et al. A compendium
596 of uniformly processed human gene expression and splicing quantitative trait loci. *Nat Genet*
597 2021;53:1290–1299. Available at: http://dx.doi.org/10.1038/s41588-021-00924-w.

598 45. Schmiedel BJ, Singh D, Madrigal A, Valdovino-Gonzalez AG, White BM, Zapardiel-Gonzalo
599 J, et al. Impact of Genetic Polymorphisms on Human Immune Cell Gene Expression. *Cell*
600 2018;175:1701–1715.e16. Available at: http://dx.doi.org/10.1016/j.cell.2018.10.022.

601 46. Gilchrist JJ, Makino S, Naranbhai V, Sharma PK, Koturan S, Tong O, et al. Natural Killer cells
602 demonstrate distinct eQTL and transcriptome-wide disease associations, highlighting their role in
603 autoimmunity. *Nat Commun* 2022;13:4073. Available at: http://dx.doi.org/10.1038/s41467-022-
604 31626-4.

605 47. Vivier E, Tomasello E, Baratin M, Walzer T, Ugolini S. Functions of natural killer cells. *Nat*
606 *Immunol* 2008;9:503–510. Available at: http://dx.doi.org/10.1038/ni1582.

607 48. Ciccia F, Accardo-Palumbo A, Alessandro R, Rizzo A, Principe S, Peralta S, et al. Interleukin-
608 22 and interleukin-22-producing NKp44+ natural killer cells in subclinical gut inflammation in
609 ankylosing spondylitis. *Arthritis Rheum* 2012;64:1869–1878. Available at:
610 http://dx.doi.org/10.1002/art.34355.

611 49. Gracey E, Vereecke L, McGovern D, Fröhling M, Schett G, Danese S, et al. Revisiting the
612 gut–joint axis: links between gut inflammation and spondyloarthritis. *Nat Rev Rheumatol*
613 2020;16:415–433. Available at: https://www.nature.com/articles/s41584-020-0454-9. Accessed
614 January 12, 2024.

615 50. Cuthbert RJ, Fragkakis EM, Dunsmuir R, Li Z, Coles M, Marzo-Ortega H, et al. Brief Report:
616 Group 3 Innate Lymphoid Cells in Human Enthesis. *Arthritis Rheumatol* 2017;69:1816–1822.
617 Available at: http://dx.doi.org/10.1002/art.40150.

618 51. Peruzzi M, Wagtmann N, Long EO. A p70 killer cell inhibitory receptor specific for several
619 HLA-B allotypes discriminates among peptides bound to HLA-B*2705. *J Exp Med*
620 1996;184:1585–1590. Available at: http://dx.doi.org/10.1084/jem.184.4.1585.

621 52. Stewart-Jones GBE, Gleria K di, Kollnberger S, McMichael AJ, Jones EY, Bowness P. Crystal
622 structures and KIR3DL1 recognition of three immunodominant viral peptides complexed to HLA-
623 B*2705. *Eur J Immunol* 2005;35:341–351. Available at: http://dx.doi.org/10.1002/eji.200425724.

624 53. Malnati MS, Peruzzi M, Parker KC, Biddison WE, Ciccone E, Moretta A, et al. Peptide
625 specificity in the recognition of MHC class I by natural killer cell clones. *Science* 1995;267:1016–
626 1018. Available at: http://dx.doi.org/10.1126/science.7863326.

627 54. Kollnberger S, Chan A, Sun M-Y, Chen LY, Wright C, Gleria K di, et al. Interaction of HLA-
628 B27 homodimers with KIR3DL1 and KIR3DL2, unlike HLA-B27 heterotrimers, is independent of
629 the sequence of bound peptide. *Eur J Immunol* 2007;37:1313–1322. Available at:
630 http://dx.doi.org/10.1002/eji.200635997.

631 55. Ridley A, Hatano H, Wong-Baeza I, Shaw J, Matthews KK, Al-Mossawi H, et al. Activation-
632 Induced Killer Cell Immunoglobulin-like Receptor 3DL2 Binding to HLA-B27 Licenses Pathogenic
633 T Cell Differentiation in Spondyloarthritis. *Arthritis Rheumatol* 2016;68:901–914. Available at:
634 http://dx.doi.org/10.1002/art.39515.

635 56. Jansen DTSL, Hameetman M, Bergen J van, Huizinga TWJ, Heijde D van der, Toes REM, et
636 al. IL-17-producing CD4+ T cells are increased in early, active axial spondyloarthritis including
637 patients without imaging abnormalities. *Rheumatology* 2015;54:728–735. Available at:
638 http://dx.doi.org/10.1093/rheumatology/keu382.

639 57. Larid G, Trijau S, Barral C, Lafforgue P, Pham T. Absence of overexpression of KIR3DL2 on
640 CD4+ T cells and NK cells in patients with axial spondyloarthritis. *Rheumatology* 2023;62:e114–
641 e116. Available at: http://dx.doi.org/10.1093/rheumatology/keac546.

642 58. Wang S, Li G, Ge R, Duan Z, Zeng Z, Zhang T, et al. Association of KIR genotype with
643 susceptibility to HLA-B27-positive ankylosing spondylitis. *Mod Rheumatol* 2013;23:538–541.
644 Available at: http://dx.doi.org/10.1007/s10165-012-0692-z.

645 59. Jiao Y-L, Zhang B-C, You L, Li J-F, Zhang J, Ma C-Y, et al. Polymorphisms of KIR gene and
646 HLA-C alleles: possible association with susceptibility to HLA-B27-positive patients with
647 ankylosing spondylitis. *J Clin Immunol* 2010;30:840–844. Available at:
648 http://dx.doi.org/10.1007/s10875-010-9444-z.

649 60. Díaz-Peña R, Blanco-Gelaz MA, Suárez-Alvarez B, Martínez-Borra J, López-Vázquez A,
650 Alonso-Arias R, et al. Activating KIR genes are associated with ankylosing spondylitis in Asian
651 populations. *Hum Immunol* 2008;69:437–442. Available at:
652 http://dx.doi.org/10.1016/j.humimm.2008.04.012.

653 61. Lopez-Larrea C, Blanco-Gelaz MA, Torre-Alonso JC, Bruges Armas J, Suarez-Alvarez B,
654 Pruneda L, et al. Contribution of KIR3DL1/3DS1 to ankylosing spondylitis in human leukocyte
655 antigen-B27 Caucasian populations. *Arthritis Res Ther* 2006;8:R101. Available at:
656 http://dx.doi.org/10.1186/ar1988.

657 62. Harvey D, Pointon JJ, Sleator C, Meenagh A, Farrar C, Sun JY, et al. Analysis of killer
658 immunoglobulin-like receptor genes in ankylosing spondylitis. *Ann Rheum Dis* 2009;68:595–598.
659 Available at: http://dx.doi.org/10.1136/ard.2008.095927.

660 63. Babaie F, Mohammadi H, Salimi S, Ghanavatinegad A, Abbasifard M, Yousefi M, et al.
661 Inhibition of ERAP1 represses HLA-B27 free heavy chains expression on polarized macrophages
662 and interrupts NK cells activation and function from ankylosing spondylitis. *Clin Immunol*
663 2023;248:109268. Available at: http://dx.doi.org/10.1016/j.clim.2023.109268.

664 64. Sun JC, Lanier LL. NK cell development, homeostasis and function: parallels with $CD8^+$ T

665 cells. *Nat Rev Immunol* 2011;11:645–657. Available at: http://dx.doi.org/10.1038/nri3044.

666 65. Cohen NR, Brennan PJ, Shay T, Watts GF, Brigl M, Kang J, et al. Shared and distinct
667 transcriptional programs underlie the hybrid nature of iNKT cells. *Nat Immunol* 2013;14:90–99.
668 Available at: http://dx.doi.org/10.1038/ni.2490.

669 66. Robinette ML, Fuchs A, Cortez VS, Lee JS, Wang Y, Durum SK, et al. Transcriptional
670 programs define molecular characteristics of innate lymphoid cell classes and subsets. *Nat*
671 *Immunol* 2015;16:306–317. Available at: http://dx.doi.org/10.1038/ni.3094.

672 67. Gutierrez-Arcelus M, Ongen H, Lappalainen T, Montgomery SB, Buil A, Yurovsky A, et al.
673 Tissue-specific effects of genetic and epigenetic variation on gene regulation and splicing. *PLoS*
674 *Genet* 2015;11:e1004958. Available at: http://dx.doi.org/10.1371/journal.pgen.1004958.

675 68. Chen L, Ge B, Casale FP, Vasquez L, Kwan T, Garrido-Martín D, et al. Genetic Drivers of
676 Epigenetic and Transcriptional Variation in Human Immune Cells. *Cell* 2016;167:1398–1414.e24.
677 Available at: http://dx.doi.org/10.1016/j.cell.2016.10.026.

678 69. Costantino F, Talpin A, Evnouchidou I, Kadi A, Leboime A, Said-Nahal R, et al. ERAP1 Gene
679 Expression Is Influenced by Nonsynonymous Polymorphisms Associated With Predisposition to
680 Spondyloarthritis. *Arthritis Rheumatol* 2015;67:1525–1534. Available at:
681 http://dx.doi.org/10.1002/art.39072.

682 70. Chen L, Ridley A, Hammitzsch A, Al-Mossawi MH, Bunting H, Georgiadis D, et al. Silencing
683 or inhibition of endoplasmic reticulum aminopeptidase 1 (ERAP1) suppresses free heavy chain
684 expression and Th17 responses in ankylosing spondylitis. *Ann Rheum Dis* 2016;75:916–923.
685 Available at: http://dx.doi.org/10.1136/annrheumdis-2014-206996.

686 71. Hanson AL, Cuddihy T, Haynes K, Loo D, Morton CJ, Oppermann U, et al. Genetic Variants
687 in ERAP1 and ERAP2 Associated With Immune-Mediated Diseases Influence Protein Expression
688 and the Isoform Profile. *Arthritis Rheumatol* 2018;70:255–265. Available at:
689 http://dx.doi.org/10.1002/art.40369.

690 72. Zhao S, Chen H, Wu G, Zhao C. The association of NLRP3 and TNFRSF1A polymorphisms
691 with risk of ankylosing spondylitis and treatment efficacy of etanercept. *J Clin Lab Anal* 2017;31.
692 Available at: http://dx.doi.org/10.1002/jcla.22138.

693 73. Xing-Rong W, Sheng-Qian X, Wen L, Shan Q, Fa-Ming P, Jian-Hua X. Role of TNFRSF1A
694 and TNFRSF1B polymorphisms in susceptibility, severity, and therapeutic efficacy of etanercept
695 in human leukocyte antigen-B27-positive Chinese Han patients with ankylosing spondylitis.
696 *Medicine* 2018;97:e11677. Available at: http://dx.doi.org/10.1097/MD.0000000000011677.

697 74. Wang R, Jaw JJ, Stutzman NC, Zou Z, Sun PD. Natural killer cell-produced IFN-γ and TNF-
698 α induce target cell cytolysis through up-regulation of ICAM-1. *J Leukoc Biol* 2012;91:299–309.
699 Available at: http://dx.doi.org/10.1189/jlb.0611308.

700 75. Neznanov N, Neznanova L, Angres B, Gudkov AV. Serologically defined colon cancer antigen
701 3 is necessary for the presentation of TNF receptor 1 on cell surface. *DNA Cell Biol* 2005;24:777–
702 785. Available at: http://dx.doi.org/10.1089/dna.2005.24.777.

703 76. Wang C-M, Jan Wu Y-J, Lin J-C, Huang L-Y, Wu J, Chen J-Y. Genetic effects of B3GNT2 on
704 ankylosing spondylitis susceptibility and clinical manifestations in Taiwanese. *J Formos Med*

705 *Assoc* 2022;121:1283–1294. Available at: http://dx.doi.org/10.1016/j.jfma.2021.09.010.

706 77. Chun S, Casparino A, Patsopoulos NA, Croteau-Chonka DC, Raby BA, De Jager PL, et al.
707 Limited statistical evidence for shared genetic effects of eQTLs and autoimmune-disease-
708 associated loci in three major immune-cell types. *Nat Genet* 2017;49:600–605. Available at:
709 http://dx.doi.org/10.1038/ng.3795.

710 78. Mu Z, Wei W, Fair B, Miao J, Zhu P, Li YI. The impact of cell type and context-dependent
711 regulatory variants on human immune traits. *Genome Biol* 2021;22:1–28. Available at:
712 https://genomebiology.biomedcentral.com/articles/10.1186/s13059-021-02334-x. Accessed
713 September 20, 2023.

714 79. Barbeira AN, Bonazzola R, Gamazon ER, Liang Y, Park Y, Kim-Hellmuth S, et al. Exploiting
715 the GTEx resources to decipher the mechanisms at GWAS loci. *Genome Biol* 2021;22:49.
716 Available at: http://dx.doi.org/10.1186/s13059-020-02252-4.

717 80. Gutierrez-Arcelus M, Rich SS, Raychaudhuri S. Autoimmune diseases - connecting risk
718 alleles with molecular traits of the immune system. *Nat Rev Genet* 2016;17:160–174. Available
719 at: http://dx.doi.org/10.1038/nrg.2015.33.

720 81. Gutierrez-Arcelus M, Baglaenko Y, Arora J, Hannes S, Luo Y, Amariuta T, et al. Allele-specific
721 expression changes dynamically during T cell activation in HLA and other autoimmune loci. *Nat*
722 *Genet* 2020;52:247–253. Available at: http://dx.doi.org/10.1038/s41588-020-0579-4.

723 82. Umans BD, Battle A, Gilad Y. Where Are the Disease-Associated eQTLs? *Trends Genet*
724 2021;37:109–124. Available at: http://dx.doi.org/10.1016/j.tig.2020.08.009.

725 83. Connally NJ, Nazeen S, Lee D, Shi H, Stamatoyannopoulos J, Chun S, et al. The missing link
726 between genetic association and regulatory function. *Elife* 2022;11. Available at:
727 http://dx.doi.org/10.7554/eLife.74970.

728 84. Mostafavi H, Spence PJ, Naqvi S, Jonathan PK. Limited overlap of eQTLs and GWAS hits
729 due to systematic differences in discovery. *bioRxiv* 2022. Available at: ;

730 85. Venken K, Jacques P, Mortier C, Labadia ME, Decruy T, Coudenys J, et al. RORγt inhibition
731 selectively targets IL-17 producing iNKT and γδ-T cells enriched in Spondyloarthritis patients. *Nat*
732 *Commun* 2019;10:9. Available at: http://dx.doi.org/10.1038/s41467-018-07911-6.

733 86. Yu H, Wu H, Zheng F, Zhu C, Yin L, Dai W, et al. Gene-regulatory network analysis of
734 ankylosing spondylitis with a single-cell chromatin accessible assay. *Sci Rep* 2020;10:19411.
735 Available at: http://dx.doi.org/10.1038/s41598-020-76574-5.

736 87. Simone D, Penkava F, Ridley A, Sansom S, Al-Mossawi MH, Bowness P. Single cell analysis
737 of spondyloarthritis regulatory T cells identifies distinct synovial gene expression patterns and
738 clonal fates. *Commun Biol* 2021;4:1395. Available at: http://dx.doi.org/10.1038/s42003-021-
739 02931-3.

740 88. Alber S, Kumar S, Liu J, Huang Z-M, Paez D, Hong J, et al. Single Cell Transcriptome and
741 Surface Epitope Analysis of Ankylosing Spondylitis Facilitates Disease Classification by Machine
742 Learning. *Front Immunol* 2022;13:838636. Available at:
743 http://dx.doi.org/10.3389/fimmu.2022.838636.

744 89. Ren C, Li M, Zheng Y, Cai B, Du W, Zhang H, et al. Single-cell RNA-seq reveals altered NK
745 cell subsets and reduced levels of cytotoxic molecules in patients with ankylosing spondylitis. *J*
746 *Cell Mol Med* 2022;26:1071–1082. Available at: http://dx.doi.org/10.1111/jcmm.17159.

747 90. Yi K, Jo S, Song W, Lee H-I, Kim H-J, Kang J-H, et al. Analysis of Single-Cell Transcriptome
748 and Surface Protein Expression in Ankylosing Spondylitis Identifies OX40-Positive and
749 Glucocorticoid-Induced Tumor Necrosis Factor Receptor-Positive Pathogenic Th17 Cells.
750 *Arthritis Rheumatol* 2023;75:1176–1186. Available at: http://dx.doi.org/10.1002/art.42476.

751 91. Pan-UKB team. Pan-UK Biobank. 2020. Available at: https://pan.ukbb.broadinstitute.org.
752 Accessed 2023.

753 92. Finucane HK, Bulik-Sullivan B, Gusev A, Trynka G, Reshef Y, Loh P-R, et al. Partitioning
754 heritability by functional annotation using genome-wide association summary statistics. *Nat Genet*
755 2015;47:1228–1235. Available at: http://dx.doi.org/10.1038/ng.3404.

756 93. Myers S, Bottolo L, Freeman C, McVean G, Donnelly P. A fine-scale map of recombination
757 rates and hotspots across the human genome. *Science* 2005;310:321–324. Available at:
758 http://dx.doi.org/10.1126/science.1117196.

759 94. Lango Allen H, Estrada K, Lettre G, Berndt SI, Weedon MN, Rivadeneira F, et al. Hundreds
760 of variants clustered in genomic loci and biological pathways affect human height. *Nature*
761 2010;467:832–838. Available at: http://dx.doi.org/10.1038/nature09410.

762 95. Leeuw CA de, Mooij JM, Heskes T, Posthuma D. MAGMA: generalized gene-set analysis of
763 GWAS data. *PLoS Comput Biol* 2015;11:e1004219. Available at:
764 http://dx.doi.org/10.1371/journal.pcbi.1004219.

765 96. Yuhan H, Stephanie H, Erica A-N, Mauck WM, Shiwei Z, Andrew B, et al. Integrated analysis
766 of multimodal single-cell data. *Cell* 2021;184:3573–3587.e29. Available at:
767 http://dx.doi.org/10.1016/j.cell.2021.04.048. Accessed May 31, 2023.

768 97. Korsunsky I, Millard N, Fan J, Slowikowski K, Zhang F, Wei K, et al. Fast, sensitive and
769 accurate integration of single-cell data with Harmony. *Nat Methods* 2019;16:1289–1296.
770 Available at: http://dx.doi.org/10.1038/s41592-019-0619-0.

771 98. Giambartolomei C, Vukcevic D, Schadt EE, Franke L, Hingorani AD, Wallace C, et al.
772 Bayesian test for colocalisation between pairs of genetic association studies using summary
773 statistics. *PLoS Genet* 2014;10:e1004383. Available at:
774 http://dx.doi.org/10.1371/journal.pgen.1004383.

775 99. Kramer NE, Davis ES, Wenger CD, Deoudes EM, Parker SM, Love MI, et al. Plotgardener:
776 cultivating precise multi-panel figures in R. *Bioinformatics* 2022;38:2042–2045. Available at:
777 http://dx.doi.org/10.1093/bioinformatics/btac057.

778 100. Liu B, Gloudemans MJ, Rao AS, Ingelsson E, Montgomery SB. Abundant associations with
779 gene expression complicate GWAS follow-up. *Nat Genet* 2019;51:768–769. Available at:
780 http://dx.doi.org/10.1038/s41588-019-0404-0.

781

782 **Table 1. Putative target genes identified by co-localization analysis**
783 **between AS-associated loci and eQTLs in NK cells.**

Lead GWAS Variant	P-value	GWAS	Putative Target Gene	Posterior probability of shared causal variant	Quantification method	eQTL study
rs27529	1.24E-40	IGAS	ERAP1	0.99186	microarray	Gilchrist et al. 2021
rs6759298	2.07E-38	IGAS	B3GNT2	0.97245	RNA-seq	Schmiedel et al. 2018
rs1128905	3.17E-10	IGAS	ENTR1	0.8207	microarray	Gilchrist et al. 2021
rs1860545	8.66E-10	IGAS	TNFRSF1A	0.99673	RNA-seq	Schmiedel et al. 2018
rs11065898	5.41E-08	IGAS	TMEM116	0.87563	microarray	Gilchrist et al. 2021
rs9619386	4.42E-07	IGAS	UBE2L3	0.96397	microarray	Gilchrist et al. 2021
rs1250542	2.07E-06	IGAS	ZMIZ1	0.87272	microarray	Gilchrist et al. 2021
rs1250542	2.07E-06	IGAS	ZMIZ1	0.83268	RNA-seq	Schmiedel et al. 2018
rs952594	2.08E-06	IGAS	APEH	0.75689	microarray	Gilchrist et al. 2021
rs952594	2.08E-06	IGAS	RBM6	0.91981	RNA-seq	Schmiedel et al. 2018
rs952594	2.08E-06	IGAS	UBA7	0.94237	microarray	Gilchrist et al. 2021
rs952594	2.08E-06	IGAS	UBA7	0.8851	RNA-seq	Schmiedel et al. 2018
rs6565217	2.82E-06	IGAS	AC135050.3	0.91556	RNA-seq	Schmiedel et al. 2018
rs6565217	2.82E-06	IGAS	STX4	0.94653	RNA-seq	Schmiedel et al. 2018
rs7191548	3.13E-06	IGAS	EIF3CL	0.7822	microarray	Gilchrist et al. 2021
rs7191548	3.13E-06	IGAS	NPIPB8	0.97545	microarray	Gilchrist et al. 2021
rs7191548	3.13E-06	IGAS	SGF29	0.85225	microarray	Gilchrist et al. 2021
rs7191548	3.13E-06	IGAS	TUFM	0.82246	microarray	Gilchrist et al. 2021
rs7191548	3.13E-06	IGAS	TUFM	0.95694	RNA-seq	Schmiedel et al. 2018
rs6583441	3.84E-06	IGAS	IKZF1	0.96244	RNA-seq	Schmiedel et al. 2018
rs4690326	6.49E-06	IGAS	DGKQ	0.91883	microarray	Gilchrist et al. 2021
rs4690326	6.49E-06	IGAS	DGKQ	0.89989	RNA-seq	Schmiedel et al. 2018
rs4690326	6.49E-06	IGAS	IDUA	0.98988	microarray	Gilchrist et al. 2021
rs4690326	6.49E-06	IGAS	SLC49A3	0.801	RNA-seq	Schmiedel et al. 2018
rs26481	9.17E-06	UK Biobank	CAST	0.95638	microarray	Gilchrist et al. 2021
rs26481	9.17E-06	UK Biobank	ERAP1	0.95565	microarray	Gilchrist et al. 2021
rs2236167	3.57E-05	IGAS	PPP2R3C	0.9491	microarray	Gilchrist et al. 2021

784

785 ## Figure legends

786 **Figure 1. Human NK cell-specific open chromatin regions are enriched in AS genetic risk.**
787 (**A**) Cartoon depicting the Calderon *et al.* study design. Peripheral blood cells from 4 healthy
788 subjects were sorted into immune cell populations that we grouped *in silico* into seven cell types
789 (see Methods). Assay for Transposase-Accessible Chromatin using sequencing (ATAC-seq) was
790 performed with and without prior *in vitro* activation. (**B**) Graphical representation of LDSC-SEG
791 analysis: identification of cell type-specific annotations (in our case open chromatin regions),
792 followed by the integration with GWAS summary statistics to obtain a risk enrichment coefficient
793 β and P-value. (**C**) Volcano plots showing results of differential accessibility analyses for each cell
794 type compared to the other cell types. Colored dots indicate open chromatin peaks in the top
795 decile of the t-statistic for each cell type, which were used for LDSC-SEG analysis. (**D-E**) Bar
796 graphs displaying the AS genetic risk enrichment coefficient β and block jackknife standard error
797 for cell type-specific open chromatin accounting for control peaks and baseline annotations.
798 Summary statistics from the International Genetics of Ankylosing Spondylitis Consortium (IGAS)
799 (**D**) and UK Biobank (**E**) GWAS were used. * indicates P < 0.05.
800
801 **Figure 2. NK cells show enrichment of cell type-specific expression of AS-associated**
802 **genes.** (**A**) Cartoon depicting the Gutierrez-Arcelus *et al.* study. Peripheral blood cells from 6
803 healthy subjects were sorted into NK cells (orange) and six T cell populations (purple): CD4+ T,
804 CD8+ T, MAIT, iNKT, and two γδ T cell populations. Bulk RNA sequencing was performed on two
805 replicates per sample. (**B**) Graphical representation of the SNPsea method illustrating the
806 integration of gene expression profiles with risk loci obtained from GWAS. (**C**) Bar graphs showing
807 -log10(P-value) for enrichment of cell type-specific expression of genes in AS risk loci using
808 SNPsea. (**D**) Heatmap showing expression levels for genes in AS risk loci that were significantly
809 upregulated in NK cells compared to six T cells subsets. Expression levels are scaled by row.
810 Tpm: transcripts per million. ** indicates P < 0.01.
811
812 **Figure 3. Human gut single-cell atlas reveals significant upregulation of AS-associated**
813 **genes in NK cells.** (**A**) Cartoon depicting the generation of the Space-Time Gut Cell Atlas with
814 samples from fetal, pediatric and adult subjects. (**B**) Graphical representation of the scDRS
815 method, which integrates GWAS risk genes with single cell data to identify disease-relevant cells.
816 (**C**) Visualization of the Space-Time Gut Cell Atlas data using UMAP on the top 20 principal
817 components from 1,997 variable genes from the scRNA-seq expression matrix. (**D**) Same UMAP
818 visualization as in C. Cells with significant scDRS score (20% FDR) are colored in red. (**E**) Bar
819 graph showing enrichment of scDRS significant cells per cell type (cell-type percent in whole
820 dataset over cell-type percent within scDRS significant cells). (**F**) Bar graph showing the number
821 of significant scDRS cells for each cell type using the fine-grained annotations from the Space-
822 Time Gut Cell Atlas. Cell populations with at least 15 significant scDRS cells are shown. (**G**)
823 Scaled average expression levels and percent of cells expressing a given gene for 50 genes
824 associated with AS that had significant upregulation (5% FDR) in NK cells compared to the other
825 cell types. Genes are sorted by multiplying their MAGMA score (strength of association with AS)
826 by their average level of expression in NK cells.
827
828 **Figure. 4. Co-localization of AS risk loci and NK cell eQTLs points to putative target genes**
829 **for AS risk variants.** (**A-D**) Manhattan plots showing AS GWAS and NK cell eQTL -log10(P-
830 values) for SNPs within 500 kb of a lead GWAS SNP. The color of each SNP indicates its level
831 of linkage disequilibrium (LD) between with the lead GWAS SNP (purple diamond). Genes in the
832 region are colored according to their posterior probability of hypothesis four (PP4), i.e. that the
833 same causal variant is shared between AS and the eQTL for that gene. (**A**) Manhattan plots
834 identifying putative target gene *ERAP1* using AS IGAS GWAS (top) and NK microarray gene

835 expression QTL (eQTL) data obtained from Gilchrist *et al*. (bottom) (**B**) Manhattan plots identifying
836 putative target gene *TNFRSF1A* using AS IGAS GWAS (top) and NK gene expression QTL
837 (eQTL) data obtained from Schmiedel *et al*. (bottom) (**C**) Manhattan plots identifying putative
838 target gene *ENTR1* using AS IGAS GWAS (top) and NK microarray gene expression QTL (eQTL)
839 data obtained from Gilchrist *et al*. (bottom) (**D**) Manhattan plots identifying putative target gene
840 *B3GNT2* using AS IGAS GWAS (top) and NK gene expression QTL (eQTL) data obtained from
841 Schmiedel *et al*. (bottom). All QTL summary statistics taken from eQTL Catalogue.
842
843 **Supplementary Figure 1. Heritability enrichment results for control traits.** (**A**) Bar graphs
844 display the genetic risk enrichment coefficient (y-axis) and standard error for cell-type specific
845 open chromatin accounting for control peaks and baseline annotations. Open chromatin data
846 were taken from the Calderon *et al*. study. Risk enrichment was assessed using GWAS summary
847 statistics for the positive control traits rheumatoid arthritis, Alzheimer's disease, systemic lupus
848 erythematosus, and the negative control trait height. Bars marked with "*" indicate $P < 0.05$, "**"
849 indicates $P < 0.01$, "***" indicates $P < 0.001$.
850
851 **Supplementary Figure 2. Single-cell disease relevant score results for control traits.** (**A**)
852 Visualization of the Space-Time Gut Cell Atlas using Uniform Manifold Approximation and
853 Projection (UMAP) on the top 20 principal components from 1,997 variable genes from the single-
854 cell RNA-seq expression matrix. Cells are colored based on the coarse cell type annotations from
855 the Space-Time Gut Cell Atlas. (**B**) Barplots shows the cell type proportions within the whole
856 Space-Time Gut Cell Atlas and within cells with significant disease relevant score (20% FDR) for
857 AS (using IGAS GWAS), Alzheimer's disease (AD) and rheumatoid arthritis (RA). (**C**) Same
858 UMAP visualization as in A, where cells with significant scDRS score (20% FDR) are colored in
859 red and non-significant cells are colored in gray, for each control trait.

Figure 1

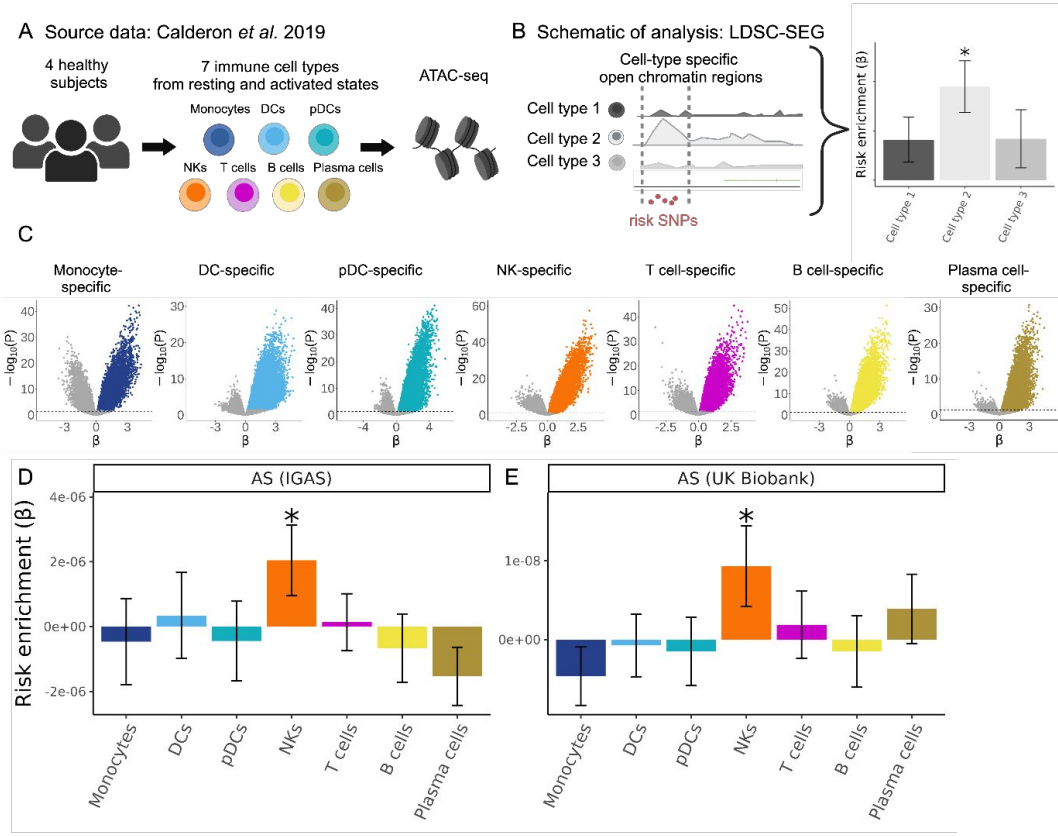
A Source data: Calderon et al. 2019
4 healthy subjects
7 immune cell types from resting and activated states
Monocytes
DCs
pDCs
NKs
T cells
B cells
Plasma cells
ATAC-seq
B Schematic of analysis: LDSC-SEG
Cell-type specific open chromatin regions
Cell type 1
Cell type 2
Cell type 3
risk SNPs
Risk enrichment (β)
Cell type 1
Cell type 2
Cell type 3
C
Monocyte-specific
DC-specific
pDC-specific
NK-specific
T cell-specific
B cell-specific
Plasma cell-specific
− log10(P)
β
D
AS (IGAS)
Risk enrichment (β)
Monocytes
DCs
pDCs
NKs
T cells
B cells
Plasma cells
E
AS (UK Biobank)
Monocytes
DCs
pDCs
NKs
T cells
B cells
Plasma cells

Figure 2

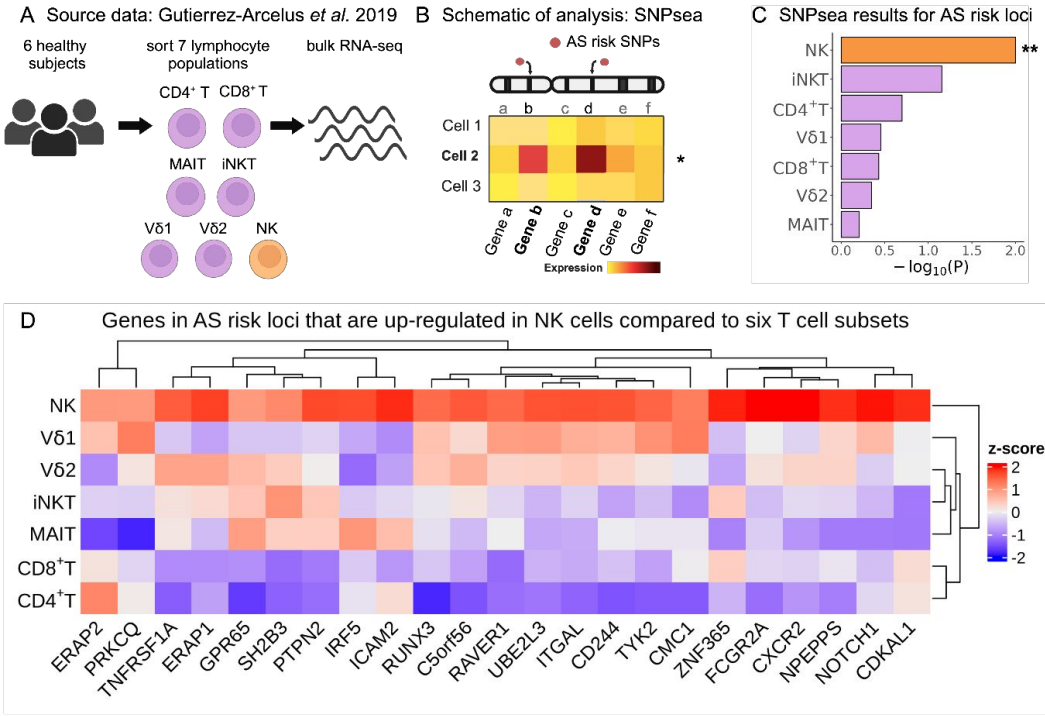
A Source data: Gutierrez-Arcelus et al. 2019
6 healthy subjects
sort 7 lymphocyte populations
bulk RNA-seq
CD4+ T
CD8+ T
MAIT
iNKT
Vδ1
Vδ2
NK
B Schematic of analysis: SNPsea
AS risk SNPs
a b c d e f
Cell 1
Cell 2
Cell 3
*
Gene a
Gene b
Gene c
Gene d
Gene e
Gene f
Expression
C SNPsea results for AS risk loci
NK
iNKT
CD4+T
Vδ1
CD8+T
Vδ2
MAIT
**
0.0 0.5 1.0 1.5 2.0
− log10(P)
D Genes in AS risk loci that are up-regulated in NK cells compared to six T cell subsets
NK
Vδ1
Vδ2
iNKT
MAIT
CD8+T
CD4+T
ERAP2
PRKCQ
TNFRSF1A
ERAP1
GPR65
SH2B3
PTPN2
IRF5
ICAM2
RUNX3
C5orf56
RAVER1
UBE2L3
ITGAL
CD244
TYK2
CMC1
ZNF365
FCGR2A
CXCR2
NPEPPS
NOTCH1
CDKAL1
z-score
2
1
0
-1
-2

Figure 3

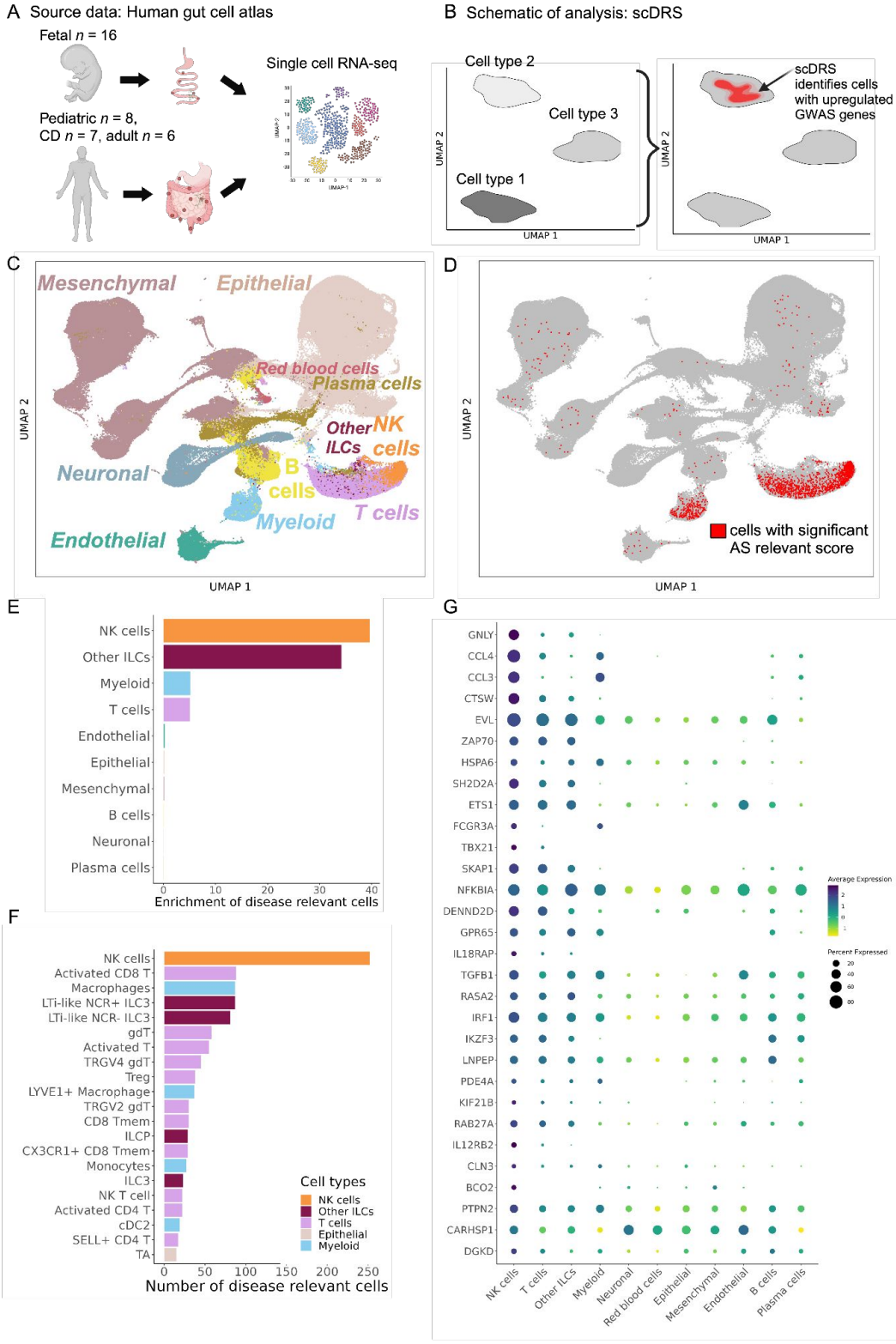
A Source data: Human gut cell atlas
Fetal n = 16
Pediatric n = 8,
CD n = 7, adult n = 6
Single cell RNA-seq
B Schematic of analysis: scDRS
Cell type 2
Cell type 3
Cell type 1
UMAP 2
UMAP 1
scDRS identifies cells with upregulated GWAS genes
C
Mesenchymal
Epithelial
Red blood cells
Plasma cells
Other ILCs
NK cells
Neuronal
B cells
T cells
Myeloid
Endothelial
D
cells with significant AS relevant score
E
NK cells
Other ILCs
Myeloid
T cells
Endothelial
Epithelial
Mesenchymal
B cells
Neuronal
Plasma cells
Enrichment of disease relevant cells
F
NK cells
Activated CD8 T
Macrophages
LTi-like NCR+ ILC3
LTi-like NCR- ILC3
gdT
Activated T
TRGV4 gdT
Treg
LYVE1+ Macrophage
TRGV2 gdT
CD8 Tmem
ILCP
CX3CR1+ CD8 Tmem
Monocytes
ILC3
NK T cell
Activated CD4 T
cDC2
SELL+ CD4 T
TA
Cell types
NK cells
Other ILCs
T cells
Epithelial
Myeloid
Number of disease relevant cells
G
GNLY
CCL4
CCL3
CTSW
EVL
ZAP70
HSPA6
SH2D2A
ETS1
FCGR3A
TBX21
SKAP1
NFKBIA
DENND2D
GPR65
IL18RAP
TGFB1
RASA2
IRF1
IKZF3
LNPEP
PDE4A
KIF21B
RAB27A
IL12RB2
CLN3
BCO2
PTPN2
CARHSP1
DGKD
NK cells
T cells
Other ILCs
Myeloid
Neuronal
Red blood cells
Epithelial
Mesenchymal
Endothelial
B cells
Plasma cells
Average Expression
Percent Expressed

Figure 4

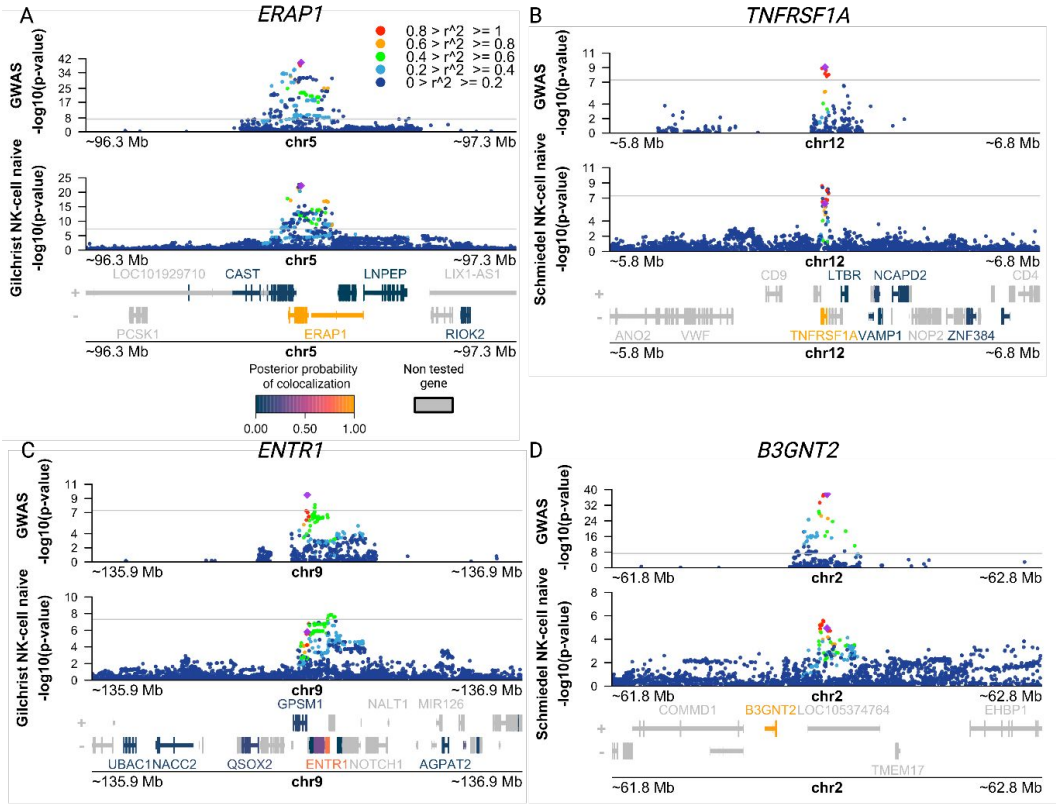
A
ERAP1
0.8 > r^2 >= 1
0.6 > r^2 >= 0.8
0.4 > r^2 >= 0.6
0.2 > r^2 >= 0.4
0 > r^2 >= 0.2
GWAS -log10(p-value)
Gilchrist NK-cell naive -log10(p-value)
~96.3 Mb
chr5
~97.3 Mb
LOC101929710
CAST
LNPEP
LIX1-AS1
PCSK1
ERAP1
RIOK2
Posterior probability of colocalization
0.00
0.50
1.00
Non tested gene
B
TNFRSF1A
Schmiedel NK-cell naive -log10(p-value)
~5.8 Mb
chr12
~6.8 Mb
CD9
LTBR
NCAPD2
CD4
ANO2
VWF
TNFRSF1A
VAMP1
NOP2
ZNF384
C
ENTR1
~135.9 Mb
chr9
~136.9 Mb
GPSM1
NALT1
MIR126
UBAC1
NACC2
QSOX2
ENTR1
NOTCH1
AGPAT2
D
B3GNT2
~61.8 Mb
chr2
~62.8 Mb
COMMD1
B3GNT2
LOC105374764
EHBP1
TMEM17

Figure S1

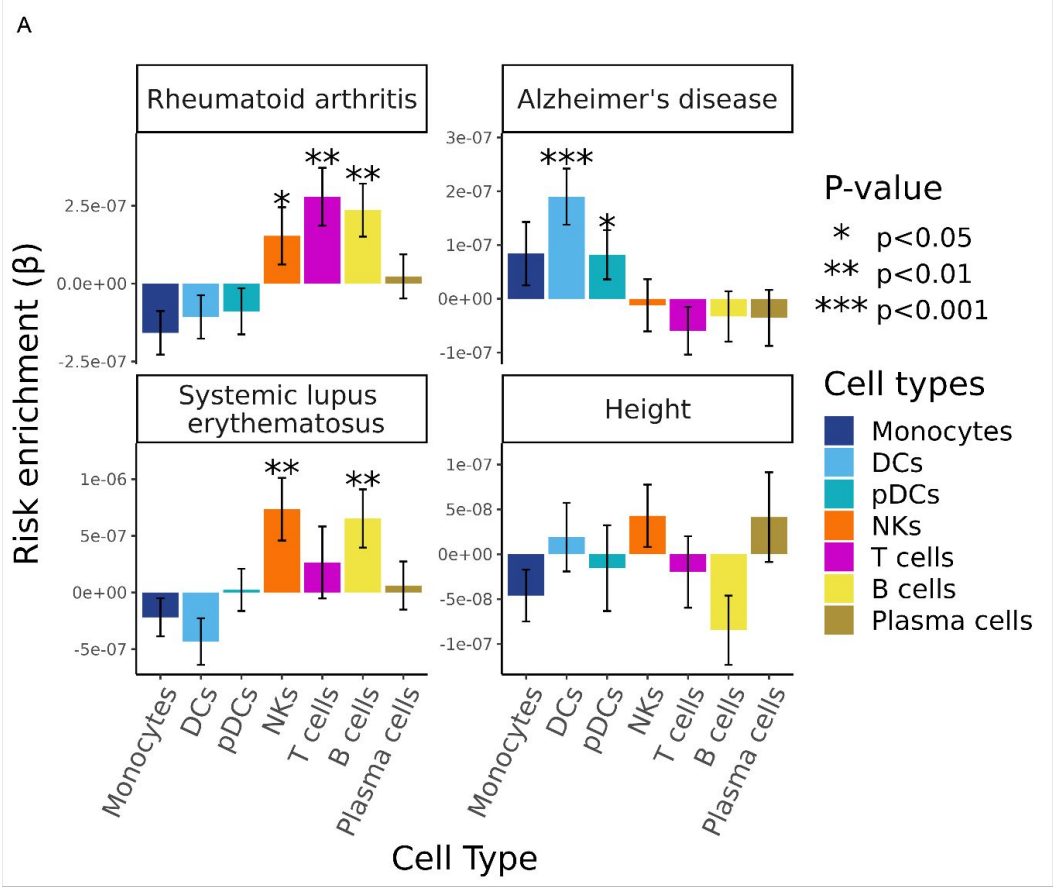
A
Rheumatoid arthritis
Alzheimer's disease
Systemic lupus erythematosus
Height
Risk enrichment (β)
2.5e-07
0.0e+00
-2.5e-07
3e-07
2e-07
1e-07
0e+00
-1e-07
1e-06
5e-07
0e+00
-5e-07
1e-07
5e-08
0e+00
-5e-08
-1e-07
*
**
***
Monocytes
DCs
pDCs
NKs
T cells
B cells
Plasma cells
Cell Type
P-value
* p<0.05
** p<0.01
*** p<0.001
Cell types
Monocytes
DCs
pDCs
NKs
T cells
B cells
Plasma cells

Figure S2

A

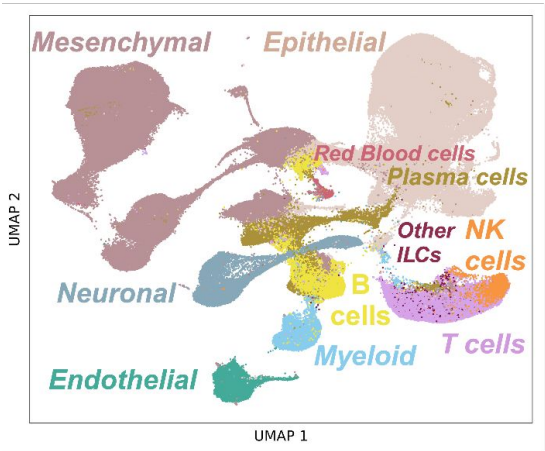

B

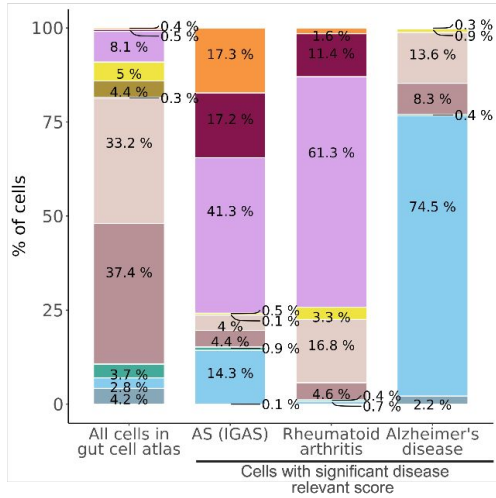
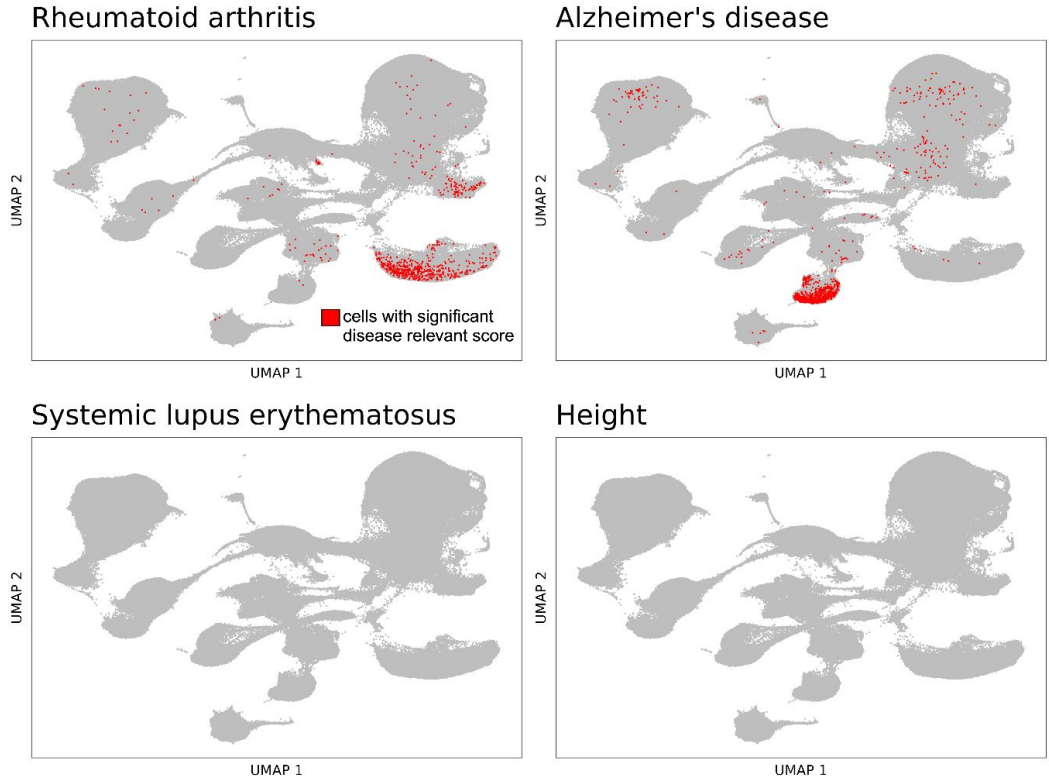
C